LA-UR-17-20911
Approved for public release; distribution is unlimited.

Title:	Comparison of particle sizes between 238PuO2 before aqueous processing, after aqueous processing, and after ball milling
Author(s):	Mulford, Roberta Nancy
Intended for:	document for record
Issued:	2017-02-06

Comparison of particle sizes between $^{238}PuO_2$ before aqueous processing, after aqueous processing, and after ball milling

Roberta N. Mulford 17 January, 2017

Particle sizes determined for a single lot of incoming Russian fuel and for a lot of fuel after aqueous processing are compared with particle sizes measured on fuel after ball-milling. The single samples of each type are believed to have particle size distributions typical of oxide from similar lots, as the processing of fuel lots is fairly uniform. Variation between lots is, as yet, uncharacterized.

Sampling and particle size measurement methods are discussed elsewhere. [1, 2]

Origin of particle samples

Particle samples were obtained from an incoming Russian $^{238}PuO_2$ fuel lot, SN175, which has been stored in the vault for about 10 years. The Russian fuel was originally precipitated in the +4 oxidation state and calcined at 950°C before shipment.

Particle samples were also obtained from an oxide lot purified by aqueous processing, PT236R. This fuel was produced from Russian fuel at Los Alamos. The Russian fuel was dissolved, precipitated in the +3 oxidation state, and calcined at 650°C to produce the $^{238}PuO_2$ in lot PT236R.

Ball-milled oxide samples were obtained from Fuel lot AQR155. Ball milling was completed on this fuel lot on May 14, 2012. The fuel lot was delivered to the sampling glovebox promptly on completion of ball milling. Particles discussed here were examined aobut 48 hours after completion of ball milling. [1]

Characteristics of particles comprising Russian fuel lot SN175

The Russian fuel lot SN175 was composed of relatively uniform small particles, with a modal diameter of 12 and with 14% of the total volume consisting of particles with a diameter smaller than 10 microns. The average diameter is 7.7 microns on a per number basis. As seen in Figure 2, the distribution of particle sizes was fairly narrow for lot SN175, with a standard deviation on the diameter of 3.15 microns.

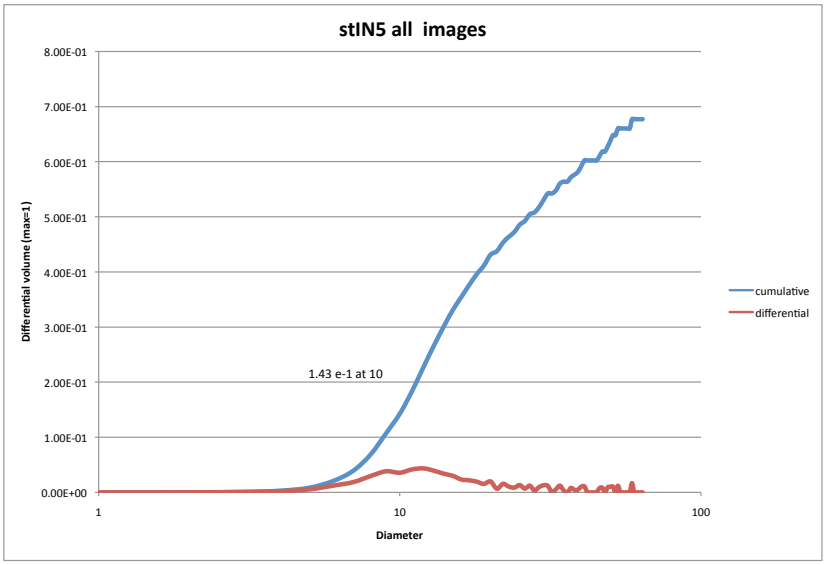

Figure 1. Cumulative histogram of particle sizes composing Russian feed fuel lot SN175.

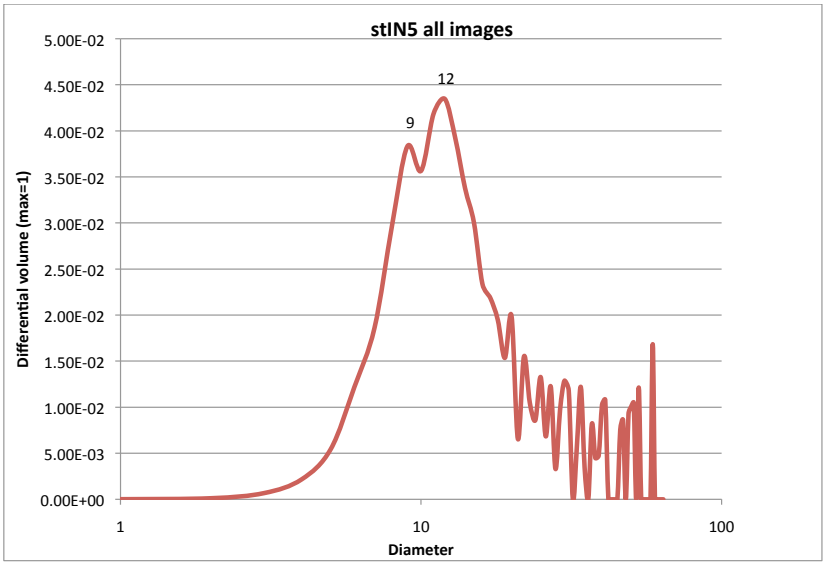

Figure 2. Russian feed fuel lot SN175 differential histogram, with particle sizes summed over 1 micron increments.

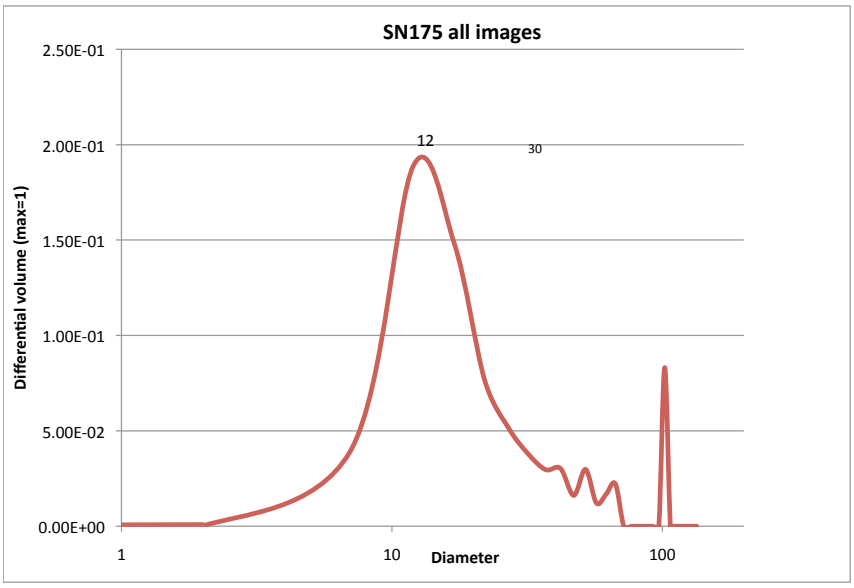

Figure 3. Russian feed fuel lot SN175 differential histogram, summed over 5 micron increments of diameter.

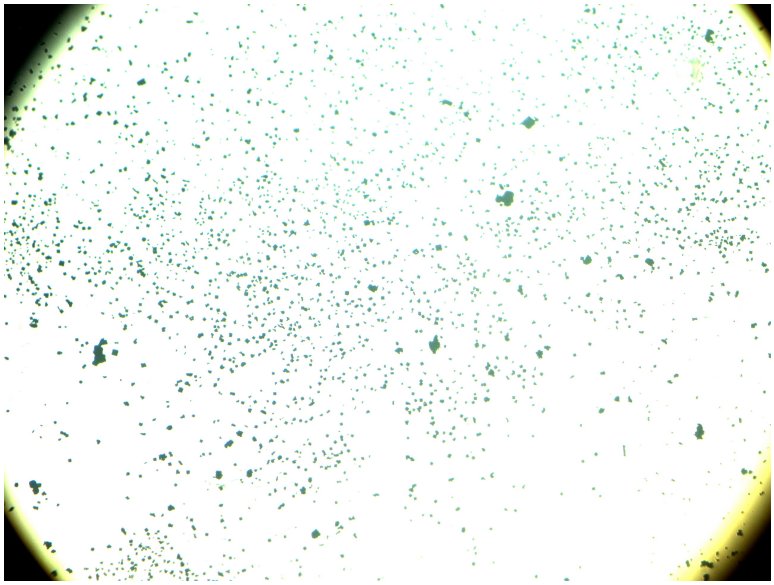

Figure 4. Typical image of particles from Russian feed fuel lot SN175.

Images of SN175 show a number of square or rectangular particles, as seen in Figure 4. Few or no needle-like particles are observed. The spherical approximation is inexact, but is a reasonable one for the majority of these particles.

Characteristics of particles comprising post-aqueous fuel lot PT236R

Fuel lot PT236R exhibited more large particles than were seen in fuel lot SN175, with an average diameter of 3.7 microns and a modal diameter of 42 microns. As seen in histograms shown in Figures 6 and 7, the distribution of sizes is quite broad and irregular, although the standard deviation of 2.8 microns on the average diameter of 3.4 microns indicates a large population around the average diameter. The average diameter is obtained on a per number basis and reflects a large number of small particles, while the modal diameter is obtained from measurements of total volume, and reflects the relatively large contribution made by large particles to the total volume of material.

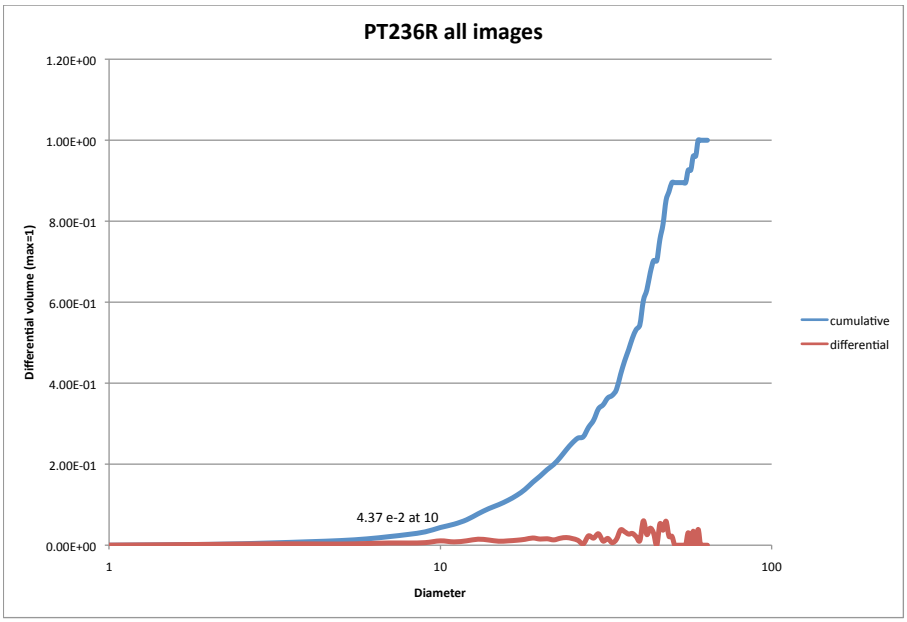

Figure 5. Post-aqueous fuel lot PT236R cumulative histogram of particle sizes

In lot PT236R, 4.37 % of the total volume consists of particles with a diameter smaller than 10 microns. In this fraction, the average diameter is 3.7 microns on a per number basis. A substantial number of particles with diameters smaller than 10 microns can be seen as a broad low peak in Figure 6, with a maximum at 3 microns, contributing to the average diameter.

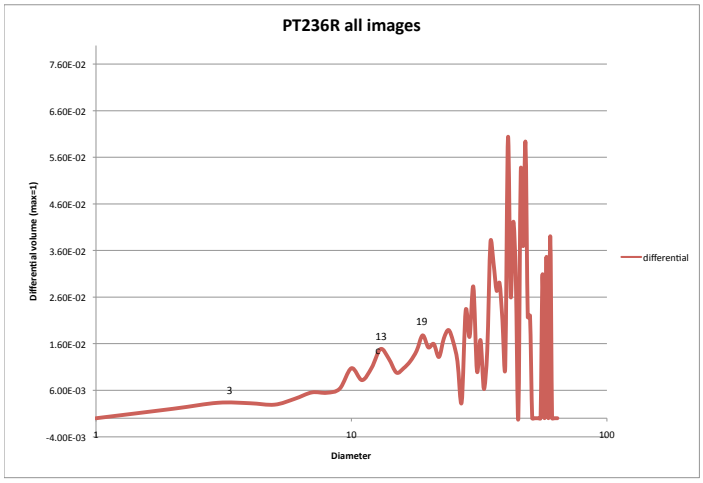

Figure 6. Post-aqueous fuel lot PT236R differential histogram, with particles summed over 1 micron increments of diameter.

The majority of the volume of the fuel is comprised of large particles, each of which contributes a substantial increment to the total volume. A smoother differential histogram can be obtained by summing over a wider interval containing larger numbers of particles, as shown in Figure 7. The modal value for this population is seen to be 42 microns.

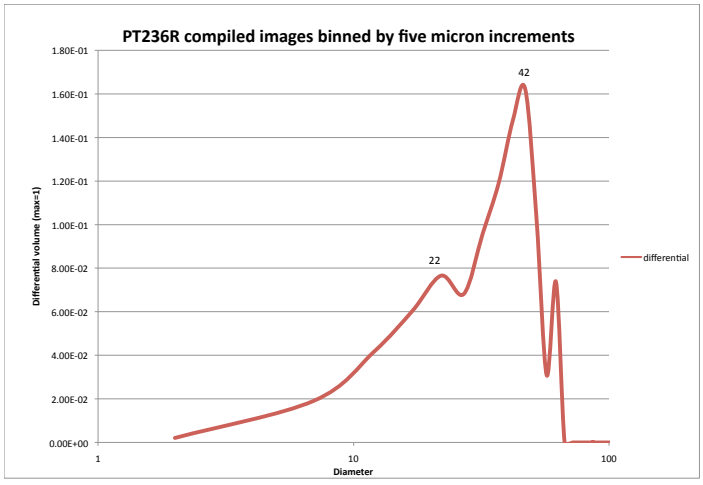

Figure 7. Post-aqueous fuel lot PT236R differential histogram smoothed by summing diameters over 5 micron increments.

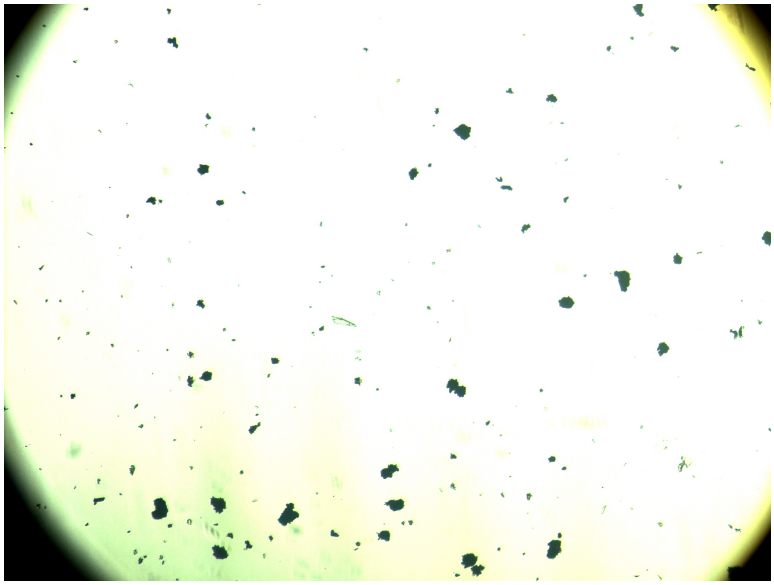

Figure 8. Typical image showing particles from post-aqueous fuel lot PT236R.

Particles produced by aqueous processing in lot PT236R are seen to have irregular shapes, as seen in Figure 8, with rough boundaries, possibly indicating agglomeration of smaller particles to produce the large particles that dominate this population.

Distributions, Ball- milled fuel

In general, the clearest images, largest number of particles, and widest range of sizes were observed at a magnification of 100x, and most data sets were taken at these magnifications. Cumulative volume fraction for the ball-milled material is shown in Figure 9.

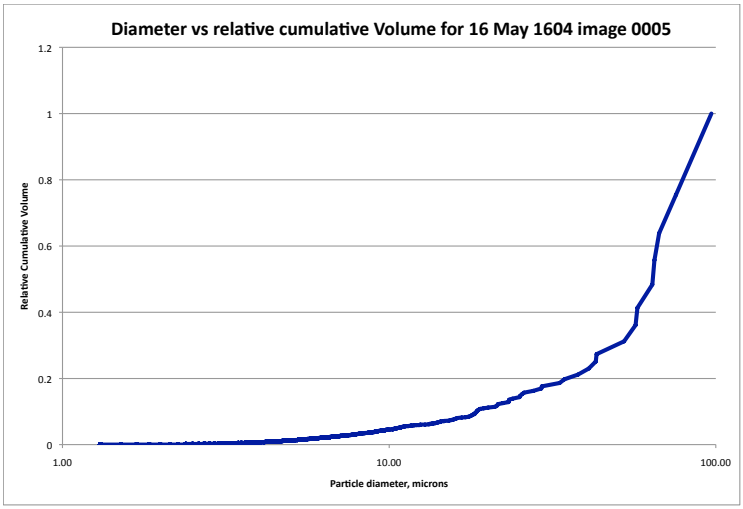

Figure 9. Cumulative volume fraction for ball-milled material aged about 48 hours.

Histograms of differential volume fraction describe the fraction of the total comprised by particles that fall within each 1μ increment of particle diameter, for individual images with between 3000 and 12000 particles.

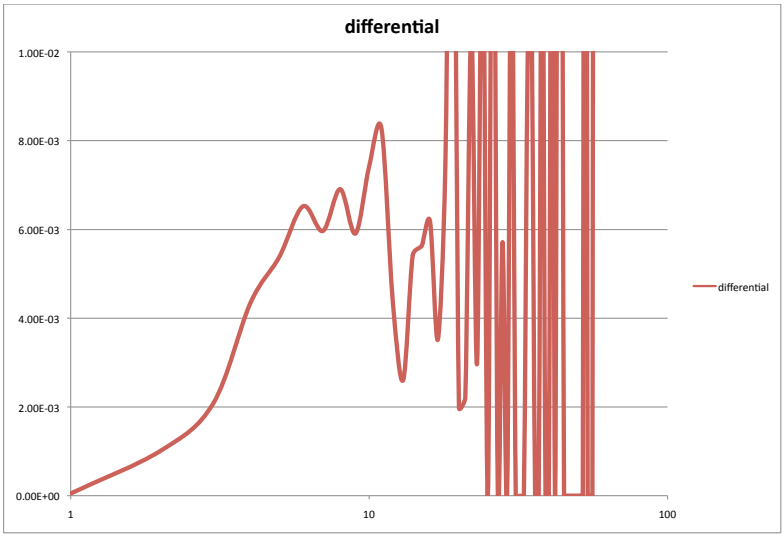

Figure 10. Histogram from one lot of ball-milled fuel after about 48 hours, showing a maximum particle size of about 10μ, with sporadic populations at larger particle sizes.

Roughness, as apparent at larger particle sizes, reflects the variation in numbers of particles of each size. The fraction comprised by a large particle is relatively large, but the number of large particles is small within each increment, so spikes appear at various sizes.

In many cases, a clear maximum is evident in the volume fraction, indicating that a particular particle size dominates in the population. In these cases, modal diameter can be used to characterize the population, as seen in Figure 11.

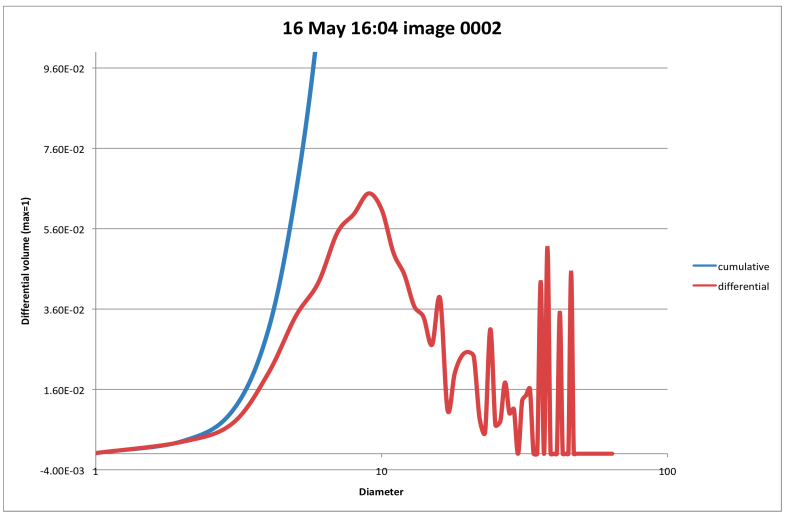

Figure 11. Histogram from a different lot of ball-milled fuel after about 48 hours, showing a modal diameter at 9μ. In many cases, a clear maximum in the volume fraction allows reporting of a modal diameter as a measurement of the particle size dominating in a particular image.

Differential volume fractions such as are shown in Figures 10 and 11 indicate the large number of small particles in the ball-milled samples.

Images of ball-milled particles

Typical images of particles at varying magnification are shown in Figures 12-16. The varying qualities of images is seen at the several magnifications used.

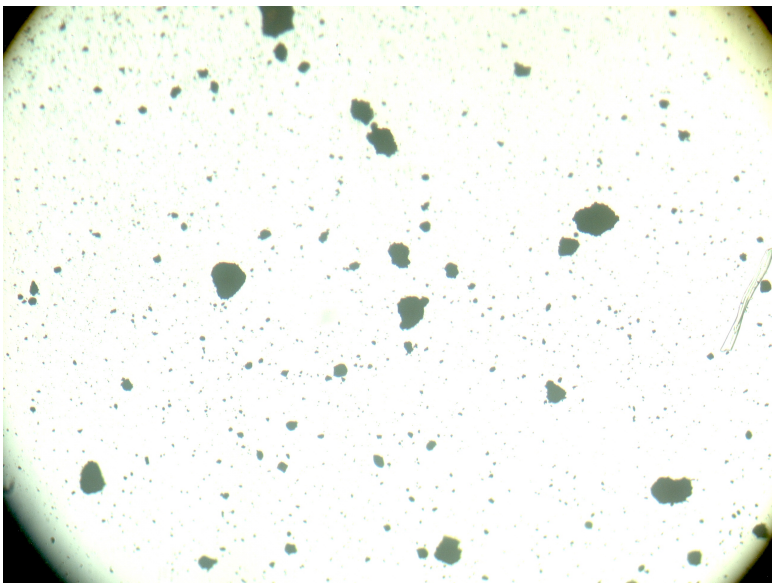

Figure 12. Image of ball-milled fuel after about 48 hours, 100x objective.

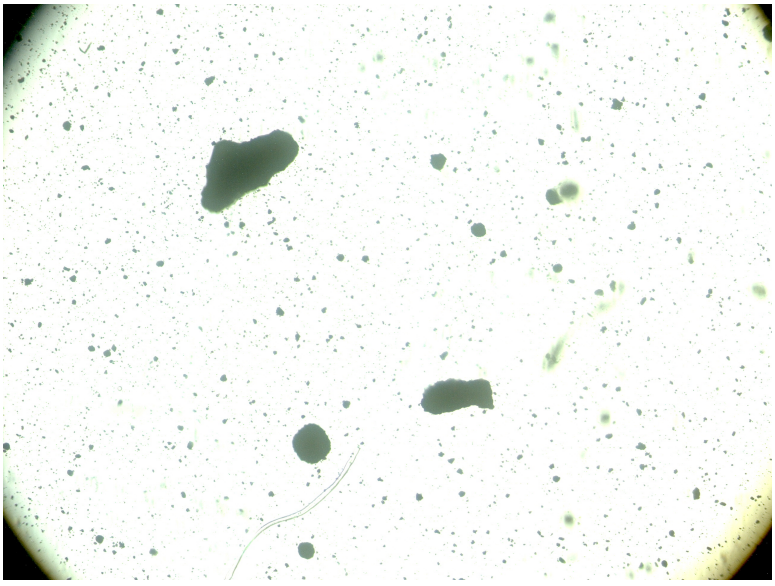

Figure 13. Image of ball-milled fuel after about 48 hours, 100x objective.

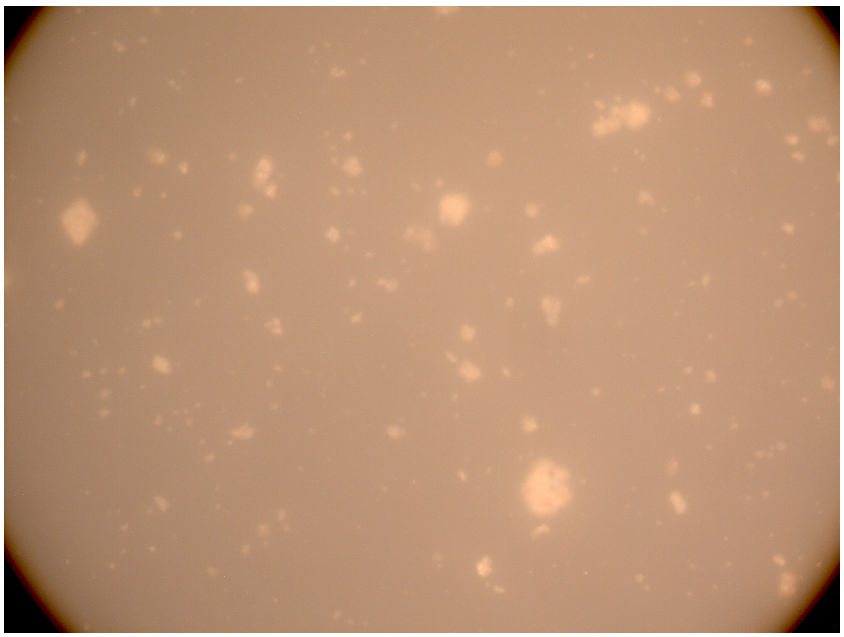

Figure 14. Image of ball-milled fuel after about 48 hours, 500x objective.

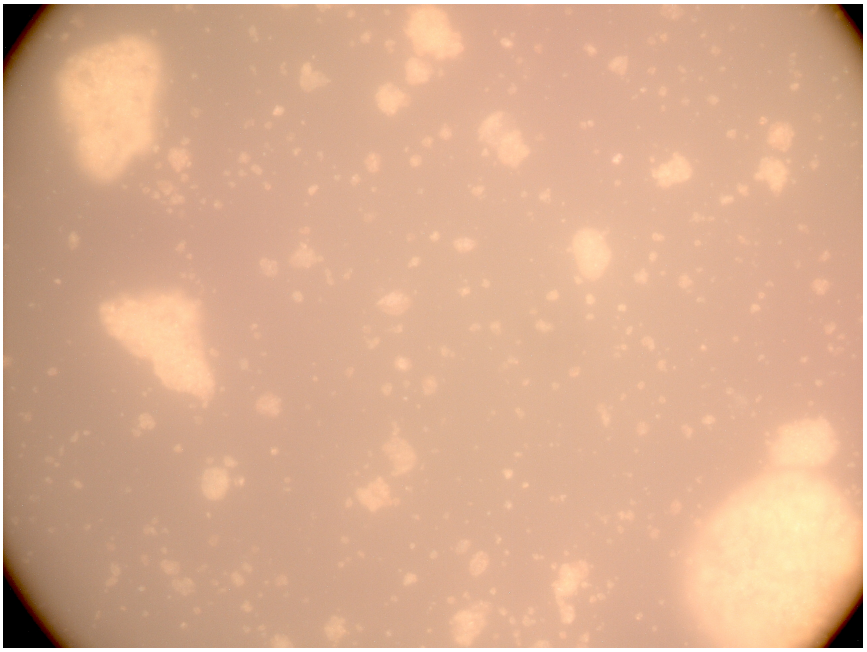

Figure 15. Image of ball-milled fuel after about 48 hours, 500x objective.

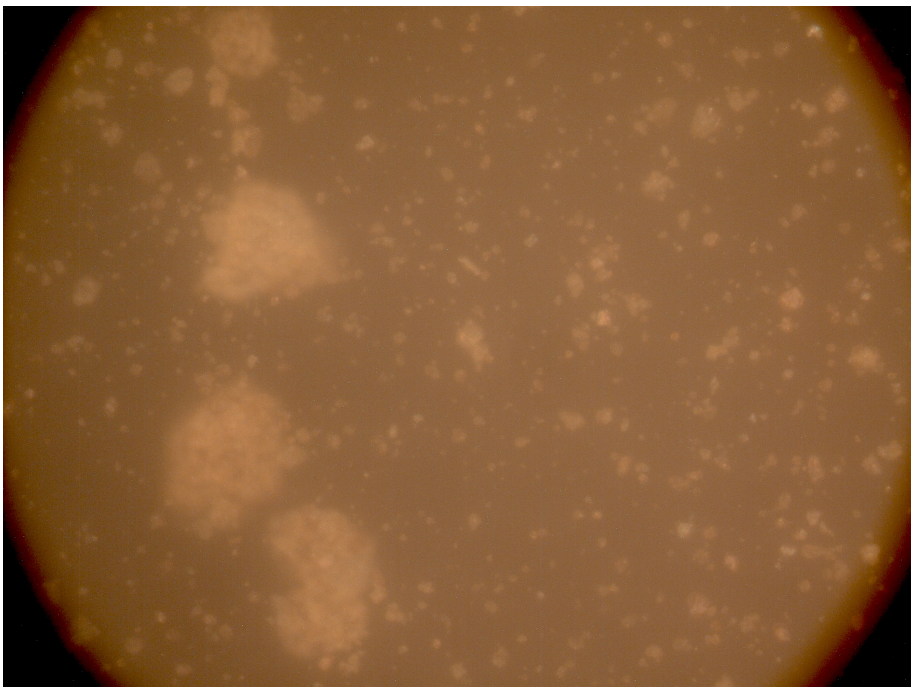

Figure 16. Image of ball-milled fuel after about 48 hours, 500x objective.

The focal plane is shallow at high magnifications, requiring a choice for the larger particles of which particular radius to image, leaving the maximum radius slightly out-of-focus for some large particles.

As seen in the Figures 12-16, the majority of particles images deviate only slightly from a circular cross-section, suggesting that the approximation of these particles as spheres in analysis of images is appropriate.

Figure 16 suggests that the larger particles may consist of agglomerations of smaller particles.

Comparison

Images of the various fuels obtained using the 100x objective are compared.

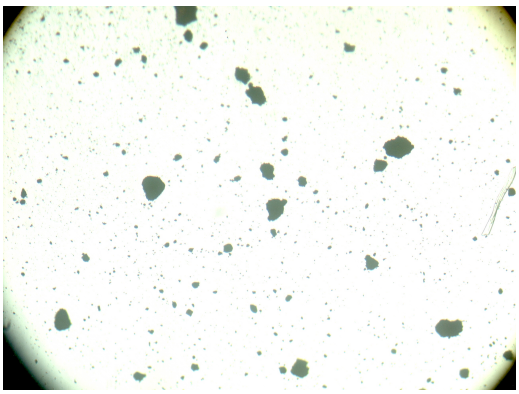

Figure 12. Ball-milled fuel after 48 hours

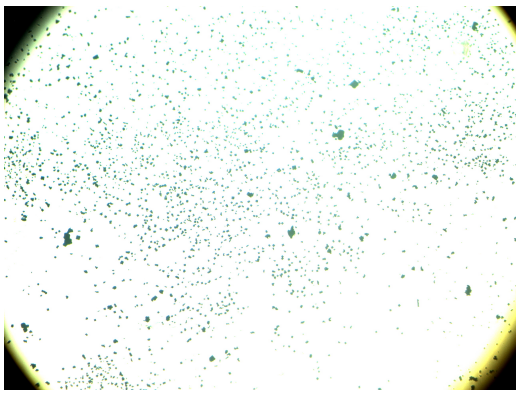

Figure 4. Image of particles from Russian feed

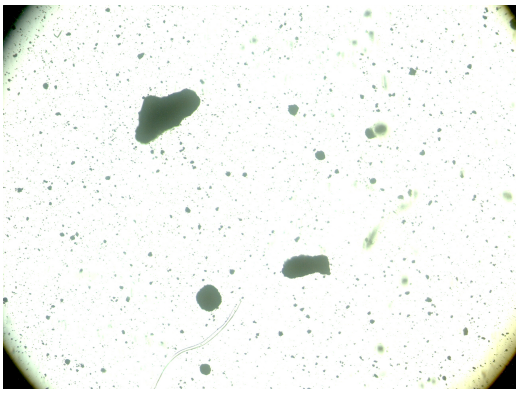

Figure 13. Ball-milled fuel after 48 hours

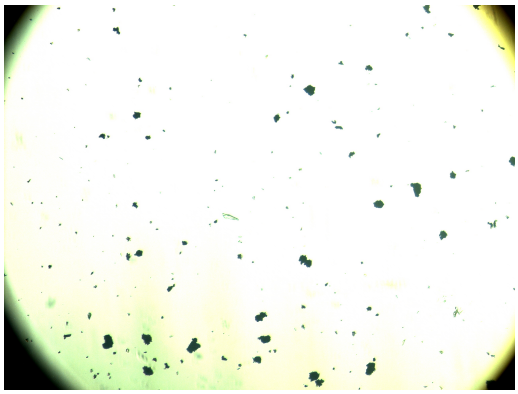

Figure 8. Fuel after aqueous processing

The large fraction of small particles is evident in both the ball-milled and the feed fuel. The images look different because there are a few large particles in the ball-milled material, which distract the eye. This fraction of small particles is absent in the fuel after aqueous processing.

Differential distributions for the several fuels are compared below.

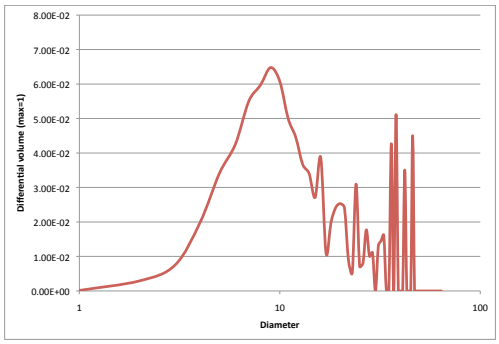

Figure 12. Particle size distribution from fuel subjected to ball milling. [1]

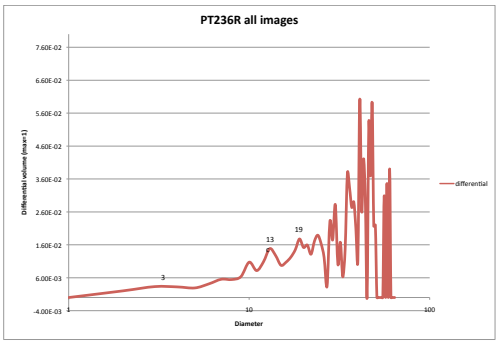

Figure 6. PT236R differential histogram, with particles summed over 1 micron increments.

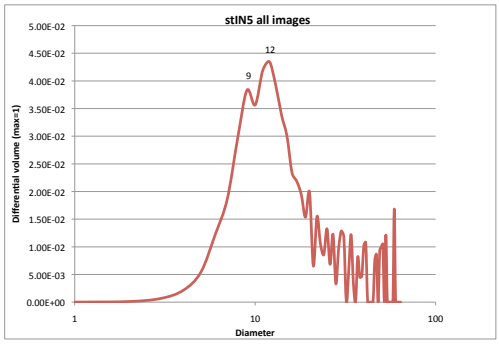

Figure 2. Fuel lot SN175 differential histogram, with particle sizes summed over 1 micron increments.

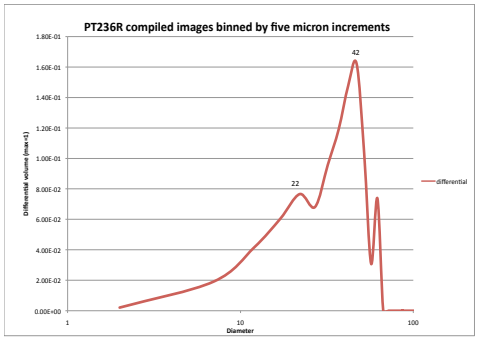

Figure 7. PT236R differential histogram smoothed by summing diameters over 5 micron increments.

Discussion

As expected, ball-milled fuel exhibited the smallest particle size, followed by the Russian feed. Aqueous processing produces a large particle size, consistent with previous observations.[4] Unanticipated large particle sizes on the order of 10μm resulting from ball-milling were inconsistent with expectations and previously reported data. [5, 6] Ball-milling is generally assumed to produce particles on the order of 1μm. [5, 6]

Russian fuel comprised of relatively small particles, 9-12μm, comparable to distributions seen in US fuel subjected to ball milling, as shown in Figure 12.

At 100x magnification, limiting acceptance to particles larger than 2 pixels imposes an effective lower limit of 1.6 μm on particles sizes reported. Such a limit is very unlikely to have influenced the distribution shown for the Russian feed, as the relatively continuous and narrow distribution argues against bimodality in the particle distribution, and gives no indication of any hidden population of very small particles in this feed. The broad distribution seen in th e post-aqueous fuel may very well have contributions from particles too small to have been measured in this experiment. A broad peak with a maximum diameter of 3 μm is visible in post-aqueous fuel, Figure 6, which might have a component with a diameter smaller than 1.6 μm. Further measurements on this batch and on similar products of aqueous processing may clarify the range of particles sizes arising from domestic aqueous processing.

The smaller particles seen in the Russian fuel may arise from any of several factors. Precipitation in the +4 oxidation state has been reported [3] to produce needle-like crystals, which may break, producing smaller particles than those typical of the original precipitate. The predominance of square particles in the image shown in Figure 4 might be attributed to broken needle-shaped crystals, but might equally suggest crystallization into cube-shaped crystals.

The Russian fuel lot has been stored as oxide for about 10 years. Helium produced within pressed material has been shown to induce intergranular fracture, resulting in fragments. [7] Similar behavior might be occurring in fuel particles. Whether individual crystals fracture as a result of autoradiolysis is not known, nor is the dependence of particle size on storage time.

Calcining temperatures differed between the feed and post-aqueous lots, with the Russian fuel calcined at 950°C and the Los Alamos product calcined at 650°C. In general, $^{239}PuO_2$ calcined at higher temperatures is expected to exhibit larger particle sizes than material calcined at lower temperatures, [8] contrary to the observations here. Size differences observed here are likely governed by oxidation state of the precipitate.

Summary

Particle size of this batch of incoming Russian $^{238}PuO_2$ fuel, after long storage, is fairly uniform, with a median size on the order of 12 μm. The distribution of sizes in fuel lot SN175 is comparable to size distributions observed in $^{238}PuO_2$ subjected to ball-milling, where the median size is between 9 μm and 10 μm. [1]

Aqueous processing appears, from this example, to have a large effect on the distribution of particle sizes, increasing the range of sizes, and increasing the population of the fine particles that are on the order of 1 μm to 5 μm. The median value is on the order of 42 μm in the fuel measured after aqueous processing. In lot PT236R, aqueous processing has produced large somewhat irregular particles that comprise most of the volume of the powder.

Ball-milled fuel is observed to have a particle size on the order of 10μm, much larger than the 1μm particle size anticipated.

Comments on Omitting Aqueous Processing of Clean Fuel Feed

The question has arisen of whether ball-milling a pellet can provide a sufficiently similar fuel to the ball-milled product of aqueous processing.

After ball-milling, the fuel is cold-pressed into a cohesive solid, or "slugged". The solid is then fragmented, sieved, and the resulting particles are sintered, some at a relatively low temperature, and some at a higher temperature. The two fractions are recombined and hot-pressed to form a pellet. These latter steps, granule production and seasoning, provide the morphology and particle size distribution that is carried into subsequent operations and hot-pressing.

The particle size distribution might differ for the ball-milled product of aqueous processing and a ball-milled pellet. Data is available for pellets fractured by a single impact. [11] Pellets less than 6 months old produce few particles smaller than 10 μm. [11] After two to five years of aging, the particle size distribution from fracture includes a larger fraction of particles with diameters less than 10 μm. [11] Ball-milling is of course a much more thorough fracturing than the single fracture that produced the 10 μm particle size. The ball-milled product from aqueous processing has a particle size of about 9 μm.

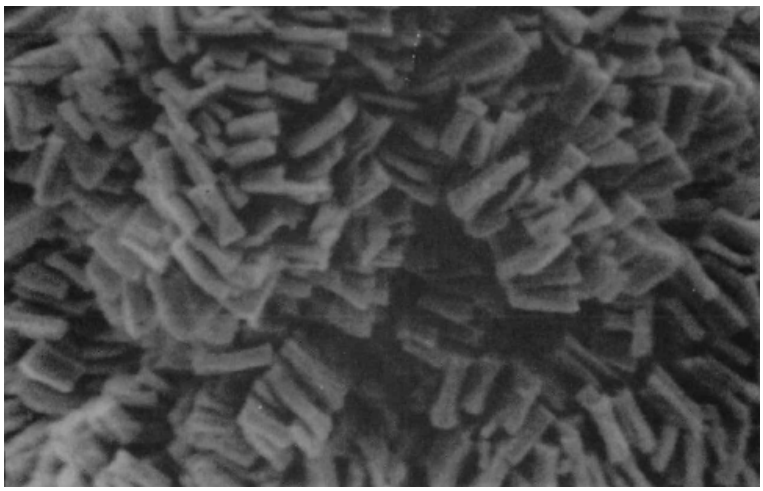

Figure 17. Surface of a $^{238}PuO_2$ particle produced from Pu(III) oxalate in a process similar to modern aqueous processing. The particle has a diameter of about 100 mm. Each "leftlet" is about 4 μm along the exposed edge.

Estimating from particles of oxide produced from Pu(III) oxalate [4] suggests that the aqueous processing naturally contains component crystallites smaller than 5 μm. The "leaflets" comprising the particle [4] are about 4 μm along the exposed edge. Thus the aqueous product lends itself to a relatively small particle size, and ball-milling is seen to produce a particle size.

Fuel obtained from a pellet is hard, and the oxide is noted for resistance to dissolution, [12] arguing for a structure with few flaws. Whether the pellet will fracture to produce a comparable particle size, or whether the consolidated fuel comprising the pellet will resist fracture must be determined by experiment.

Surface energy affects the cohesiveness of the fuel. The Russian fuel feed has a low surface energy, consistent with other observations of oxide obtained from Pu(IV) oxalate. [3, 4] Direct processing of this fuel is known to produce an incoherent pellet. [10]

Post ball-milling, images (Figures 14-16) taken at high magnification indicate loosely agglomerated particles. The particles do not appear to exhibit a well-defined crystal habit. Agglomeration of these particles suggests high surface energy, although that relatively high surface energy is commensurate with the large surface area of these small particles.

After aqueous processing, surface energy is known, historically, to be large in material precipitated as Pu(III) oxalate. [4] This energy results from a highly convoluted surface, as shown in Figure 17. A large fraction of the convolution of these pellets is retained after sintering. [4] Whether this high surface energy can be carried through granule formation and seasoning is not known, but the unusually low bulk and tap densities of these fuels [9] suggest that some degree

of convolution or porosity is preserved. Agglomeration of the high-fired fuel from day to day [10] gives further credence to the preservation of features leading to a high surface energy, even after high-firing.

The hot pressing and sintering involved in production of the pellet may be expected to reduce the surface energy of oxide in the pellet below energies seen for the other fuel forms in the processing scheme. Whether ball-milling will reduce the size of the particulate sufficiently to raise the surface energy to a value comparable to ball-milled product of aqueous fuel can only be determined by experiment.

While several factors suggest that ball-milling the consolidated fuel obtained from a pellet will produce a fuel with a larger particle size and a smaller surface energy than the ball-milled product of aqueous processing, only experiment will determine whether the anticipated differences between the fuels are significant in determining the behavior of this fuel in subsequent pellet production steps.

References

1. Roberta Mulford, Brian Berger, and Rene Chavarria, "Particle Size in Ball-milled $^{238}PuO_2$ as a Function of Residence Time in Fuel Container," Los Alamos internal report, LA-CP-12-01240, 2012.

2. Roberta N. Mulford, "Comparison of particle sizes between $^{238}PuO_2$ lots SN175 and PT236R" Los Alamos National Laboratory, LA-CP-13-00016, 2013.

3. S. Grandjean, L. De Almeida, F. De Bruycker, B. Arab-Chapelet, I. Jobelin, F. Abraham, and F. Patisson, "New insights on the reaction mechanisms of conversion of Pu-based oxalates into oxide", in proceedings of the Plutonium Futures 2012, Cambridge, UK, July 2012.

4. G.A. Burney and J.W. Congdon, "Direct Fabrication of 238Pu)2 Fuel Forms," Savannah River Laboratory, DR-942, 1982.

5. W.J. Maraman, R.A. Kent, C.E. Frantz, C.C. Land, T.H. Feiertag, G.H. Rinehart, and W.A. Stark, "Milliwatt Generator Project, April-September 1981,"Los Alamos National Laboratory, LA-9170-PR, 1981.

6. Tim George, Los Alamos National Laboratory, private communication.

7. Danièle Roudil, Jessica Bonhoure, Raphaël Pik, Michel Cuney, Christophe Jégou, and F. Gauthier-Lafaye, J. of Nucl. Mats 378 (2008) 70–78.

8. Dave Wayne, Los Alamos National Laboratory, private communication.

9. Roberta Mulford and Diane Spengler, "Bulk and Tap Densities of two granular plutonium-238 oxide fuel lots," submitted to the Proceedings of the Institute of Nuclear Materials Management 57th Annual Meeting, Atlanta, Georgia, July 2016. (LA-UR-16-24660)

10. Jeff Huling, Los Alamos National Laboratory, private communication (2012).

11. Roberta Mulford, "Plutonium-238 Oxide Fuel Fracture Behavior as a Function of Age," in Proceedings of the Institute of Nuclear Materials Management 55th Annual Meeting, Atlanta, Georgia, July 2014. (LA-UR-14-25228)

12. Lia Brodnax, Los Alamos National Laboratory, private communication (2017).